

A Novel Location Strategy for Minimizing Monitors in Vehicle Emission Remote Sensing System

Yu Kang, *Senior Member, IEEE*, Zerui Li, Yunbo Zhao, *Senior Member, IEEE*, and Jiahu Qin, *Member, IEEE*

Abstract—The vehicle emission remote sensing system is one promising solution to monitor the emissions of on-road vehicles that contribute to the air pollution in urban areas. To implement such a system an effective location strategy to place the monitors is yet to be designed. To this purpose we formulate a novel location problem where the minimum subset of roads on which traffic emission monitors are located is to be found only using the topological structure and some other available information of the traffic network. We solve this problem by transforming it into a graph-theoretic problem and considering more characteristics such as the traffic regulations and limits. After modeling the real-world traffic network as a digraph, a two-step algorithm is developed. The first step is to find all directed circuits to establish hypergraph-based set of directed circuits using the depth first searching strategy. In the second step, an approximation algorithm is designed to find the greedy transversal which is a subset of roads to place vehicle emission monitors in order to cover all the traffic circuits. The performance of the location strategy is validated by both theoretical developments and illustrative examples.

Index Terms—Intelligence transportation, location strategy, urban air pollution, vehicle emission monitor.

I. INTRODUCTION

IT IS a trend that in recent years more and more motor vehicles have been increasingly used in the urban area while high-polluting factories are being outmigrated, making vehicle emissions one of the leading factors in urban air pollution. These emissions contain large quantities of CO,

Manuscript received June 9, 2016; accepted July 27, 2016. Date of publication February 6, 2017; date of current version March 15, 2018. This work was supported in part by the National High-Tech Research and Development Program of China (863 Program 2014AA06A503), in part by the National Natural Science Foundation of China under Grant 61422307, Grant 61473269, Grant 61673350, and Grant 61673361, in part by the Scientific Research Staring Foundation for the Returned Overseas Chinese Scholars and Ministry of Education of China, in part by the Fundamental Research Funds for the Central Universities under Grant WK2100100023, in part by the Youth Innovation Promotion Association, in part by the Chinese Academy of Sciences, in part by the Youth Top-Notch Talent Support Program, in part by the 1000-Talent Youth Program, and in part by the Youth Yangtze River Scholar. This paper was recommended by Associate Editor Z. Li. (Corresponding author: Yu Kang.)

Y. Kang is with the Department of Automation, State Key Laboratory of Fire Science and Institute of Advanced Technology, University of Science and Technology of China, Hefei, China, and also with the Key Laboratory of Technology in GeoSpatial Information Processing and Application System, Chinese Academy of Sciences, Beijing, China.

Z. Li and J. Qin are with the Department of Automation, University of Science and Technology of China, Hefei, China.

Y. Zhao is with the College of Information Engineering, Zhejiang University of Technology, Hangzhou, China.

Color versions of one or more of the figures in this paper are available online at <http://ieeexplore.ieee.org>.

Digital Object Identifier 10.1109/TSMC.2016.2607221

HC, NO_x, PM, and many other kinds of toxic substances. The resulting atmospheric haze and photochemical smog then cause respiratory diseases like bronchitis and asthma, and cardiovascular diseases like stenocardia and coronary heart diseases. Living near a major traffic road is reported to increase greatly the risk of wheezing illness, lung disease, and deep vein thrombosis [1]–[3]. Such air pollution caused by vehicle emissions may thus lead to environmental failure [4]–[6].

Among all the vehicles, the *yellow-labeled cars* are the worst in terms of air pollution. It is shown that the amount of NO_x emitted by yellow-labeled cars accounts for 45.4% of all the emission, and the proportion for HC, CO, and PM is 49.1%, 47.4%, and 74.6%, respectively, in 2014 despite their 6.8% share of all vehicles in the 2015 annual report of the Ministry of Environmental Protection of China [7]. In this paper, it is noted that the whole vehicle emission pollution reduced by 0.5% although the sales quantity of cars achieved 23.5 million in 2014, which may owe to the rigid regulations on yellow-labeled cars. It shows that we are badly in need of tools that can quantitatively measure the emission effects of in-use vehicles and recognize the high-emitters.

The conventional detection methods for vehicle emissions are nonloading test (under conditions of idle speed and double idle speed) and the driving mode test, which measure the emission by simulating vehicles' running states. But in consideration of the effects on emissions of weather, traffic condition, degree of aging, and even driving habit, a great difference may exist between the simulation results and the real emissions. Furthermore, these conventional methods cannot capture the real-time emission effectively. So some advanced techniques are developed for measuring the emissions, such as the portable emission measurement system, the remote sensing system (RSS) and the on-board diagnostic technology. Using remote sensing to measure vehicle emissions started from the 1980s. In 1988, scientists from the University of Denver applied the nondispersive infrared technology to detect CO, CO₂, and HC in the tail gas in USA, and in the 1990s, the nondispersive ultraviolet technology was employed to detect NO_x [8]–[10]. It has been proved that remote sensing is an effective technology to measure real vehicle emissions and recognize high-emitters after decades of research and practice.

As an essential part in the vehicle emission monitoring system, remote sensing can conduct a preliminary screening toward thousands of vehicles when they are up and running,

thus making the vehicle emission RSS critically important. Such a system is formed with traffic emission monitors set on the roads, by which the emission from large quantity of vehicles passing through the monitors can be measured in real time. There is no doubt that the amount and location of the monitors have an significant influence on the monitoring performance. Since the amount of monitors is constrained by the economic considerations, the optimal location of monitors thus becomes a critical technique for the vehicle emission RSS.

The location problems in the transportation domain are usually studied to observe, estimate, and predict link, O/D, and route flows [11], [12], with passive or active traffic sensors [13]–[15]. A majority of them focus on the determination of the minimum amount of required traffic counters or the optimal locations of a certain amount of traffic counters, to achieve a better estimation of the O/D matrix. Lam and Lo [16] provided a first formal method for the problem regarding traffic flow. Several heuristic methods were proposed to meet the challenge. Ehlert *et al.* [17] proposed two solutions by means of integer linear programming: one solution takes existing detectors on the network into consideration, and the other takes flow information from the prior O/D into consideration. Yang *et al.* [18], [19] proposed four location rules, and developed several models based on integer linear programming, and designed heuristics to obtain the links required to be counted in the traffic network that satisfy the four rules. Bianco *et al.* [20], [21] extended this problem through considering conditions on the location of traffic counters at vertices, making it possible to decide the flow of the whole network uniquely. Gan *et al.* [22], [23] made a comprehensive research on the traffic counters location, error bound and estimation method in an integrated approach, and then demonstrated some properties of the different location rules.

The location problems are also addressed directly to infer flows of the unobserved links. Hu *et al.* [24] explained how to decide the minimum subset of links for traffic counters' deployment to derive flows of the other links in the traffic network, by describing the network using a matrix revealing the link-path incidence. In order to eliminate the requirement for enumerating all paths in Hu *et al.*'s [24] work, Ng [25] reformulated the problem of link observability to enumerate nodes instead of paths. Bianco *et al.* [26] presented an exact branch and bound approach for this problem, based on a binary branching rule, to obtain bounds on the solution value. They also applied a genetic approach to find good quality solutions. Gu *et al.* [27], [28] treated this problem as a traffic control problem, which is aimed to determine a minimum edge control set through modeling the traffic network as a digraph, showing that for a strongly connected directed graph, if the digraph has m edges and n vertices, we need to deploy $m - n + 1$ sensors in order to decide the traffic flows of this digraph uniquely. Based on these results Lin and Xu [29] had a further study and proposed a more general location strategy for traffic network by taking the unbalanced nodes into consideration. What is more, the k -monitor problem was proposed by Yan [30] and Chin *et al.* [31] which is to determine a set containing k edges with monitors on them such that the amount

of edges with the traffic flows determined is maximized. This problem was proven to be NP-hard and its approximation algorithms with polynomial-time complexity were developed.

In transportation sensors are usually used to observe or estimate the O/D flows, route flows or link flows. On the contrary here we are interested in finding the minimum subset of roads on which traffic emission monitors are placed to monitor vehicles under certain conditions. While some characteristics of roads, like traffic flow, geographic position, and congestion situation, are useful to decide whether a monitor should be located or not, it is intractable to quantify these influencing factors such as geographic position and congestion situation, and information like traffic flow of the whole road network is not easily accessible even for the national traffic administrative department. In this paper, we try to study the possibility of resolving this problem only using the topological structure and some other available information of the traffic network. We propose a two-step algorithm using both depth first searching and greedy strategy to find the minimum set of roads with traffic emission monitors, based on the digraph modeled from the traffic network.

The structure of the remaining content in this paper is as follows. In Section II, we introduce the vehicle emission RSS and discuss how to obtain the graph-based urban road network and convert the location problem to a graph-theoretic problem. We then present a two-step location strategy with performance analysis in Section III. The proposed strategy is validated with both simulation example and real-world tests in Section IV. The summary to this paper will be presented at the last section.

II. PRELIMINARIES

In this section, we first give a brief introduction to the vehicle emission RSS, which is to be established according to the location strategy developed in this paper, then model the road network, the object of locating detectors, and finally formulate the problem of interest based on the model.

A. Vehicle Emission Remote Sensing System

Vehicle emissions are conventionally detected by using the so-called vehicle emission field testing station, an offline and contacting method for measuring emissions, which is of high accuracy but low efficiency. The vehicle emission RSS studied in this paper is a complementary method for the field testing station, which is composed of the vehicle emission monitors distributed onto the traffic network. It can be used to separate the yellow-labeled cars out for further detection by field testing station. Here, the monitors in this system can measure gaseous pollutants from vehicles driven in all lanes of the road simultaneously, including CO, CO₂, HC, and NO, as well as the opacity of exhaust, which is an important index for diesel-engined vehicles.

The monitors use the tunable diode laser absorption spectroscopy technology to measure CO and CO₂, and differential optical absorption spectroscopy technology for HC and NO. The infrared or ultraviolet light beams projected by the light

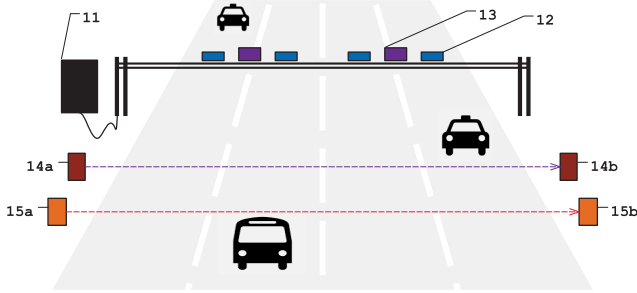


Fig. 1. Traffic emission monitor. Eleven represents the industrial controller. Twelve and thirteen are the video cameras and the license recognizer. Fourteen and fifteen located on road sides are the emission detector and the speed/acceleration sensor, respectively.

source are to measure CO, CO₂, HC, and NO, respectively. The relationship between the attenuation of light intensity and the concentrations of gases can be expressed as follows, which is referred to as Beer-Lambert law:

$$T = I_{(\lambda)}/I_{0(\lambda)} = \exp(-\beta cL)$$

where $I_{0(\lambda)}$ and $I_{(\lambda)}$ represent the light intensities of the projected beam by the light source and the received one after traveling L , β is the atmospheric attenuation coefficient, and c is concentration of a certain gas. The opacity of exhaust can also be measured by the monitor. When a diesel-engined vehicle passing through a monitor, the laser beam from light source on one side of the road is received by the receiver, whose intensity is determined by the shading ability of the exhaust, then the opacity can be worked out using light transmittance measurement principle.

However, to obtain more complete measurement, the concentrations of CO, CO₂, HC, and NO and opacity of exhaust should be fused with other data, e.g., speed, acceleration, and meteorology, with the aid of speed/acceleration sensor, cameras, and so on. Fig. 1 is a diagram of vehicle emission monitor, which consists of an emission detector, a speed/acceleration sensor, a license recognizer, an industrial controller, video cameras, and other corollary equipments. Fig. 2 is a site installation drawing of the monitor.

B. Road Network Modeling

In this part, we will establish the model of traffic network, based on which the location strategy is developed. And first some necessary graph-theoretic definitions are given as follows, most of which are from [46] and [47].

A *digraph* is an organized pair $D = (V(D), A(D))$ composed of a set $V := V(D)$ and a set $A := A(D)$, where V is a finite set of *vertices* and A is the set of *arcs*, which are unilateral relations on V . The number of vertices and arcs in D are called to be the *order* and *size* of D , respectively, denoted by $|V|$ and $|A|$. Define another digraph $D^*(V(D^*), A(D^*))$. $V(D^*)$ is equal to $A(D)$ and the vertices in D^* are adjacent iff the corresponding arcs in D are incident. The digraph D^* is referred to as the *line digraph* of D .

A *directed walk* of the digraph D is an alternate sequence $W = (v_0, a_1, v_1, \dots, a_\ell, v_\ell)$, in the sequence v_{i-1} is the tail of

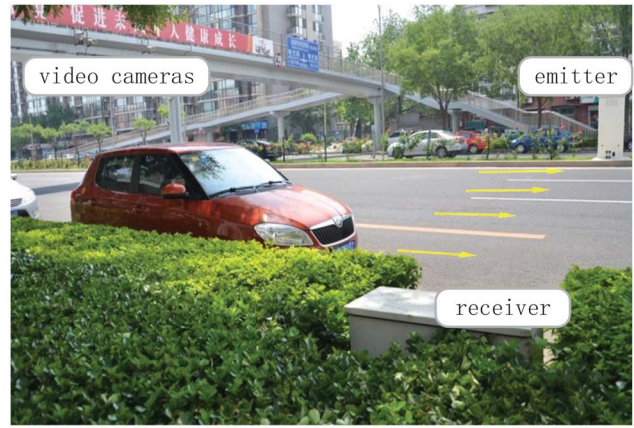


Fig. 2. Site installation of the traffic emission monitor. The emitter projects infrared and ultraviolet lasers, which are then received by the receiver on the other side, to measure the concentrations of CO, HC, and NO and also the speed and acceleration of the passing vehicle.

a_i and v_i is the head of a_i , $1 \leq i \leq \ell$ where the integer ℓ is the *length* of the walk. Usually the arcs a_i are dropped. Here the vertex v_0 and v_ℓ are the *origin* and *terminal*, respectively. Let *directed* (x, y) -*walk* denote a walk from x to y , then the vertex y is said to be *reachable* from the vertex x . A digraph is referred to be *strongly connected* if any two vertices in the digraph are reachable from each other. A directed walk is said to be a *directed trail* (or *directed path*) if it has distinct arcs (or distinct vertices). A directed trail (or directed path) is said to be a *directed circuit* (or *directed cycle*) if it has an identical origin and terminal.

A *set system* is a pair of (V, \mathcal{F}) . V is a finite set. $\mathcal{F} \subset 2^V$ is a family of subsets of V . If \mathcal{F} is composed of pairs elements of V , the set system is a graph without loop. Therefore the set system can be considered as generalizations of graphs, which are usually known as *hypergraphs* denoted by $H = (V(H), \mathcal{F}(H))$. In the hypergraph, $V := V(H)$ is called the *vertex set* of H , and $\mathcal{F} := \mathcal{F}(H)$ the *hyperedge set*. The definitions of *order* and *size* also exist in the hypergraph, denoted by $|V|$ and $|\mathcal{F}|$, respectively. A hypergraph is called to be a *simple hypergraph* if it has no repeated edges such that $F_i \subseteq F_j \Rightarrow i = j$. The star $H(x)$ centered in vertex x is the family of hyperedges containing x , and its cardinality of hyperedges are called *degree* symbolically by $d(x)$. The maximal degree of a hypergraph H is denoted by $\Delta(H)$. Let T denote a *transversal* of hypergraph $H = (V(H), \mathcal{F}(H))$. T is a subset of V which meets every edge, i.e., $T \cap F_i \neq \emptyset$ for all $F_i \in \mathcal{F}$. If T 's any proper subset is not a transversal, T is considered as a *minimal transversal*. Use \mathcal{T} to represent the set containing all minimal transversals in the hypergraph H . Then the transversal with minimum cardinality is said to be the *minimum transversal*.

With the definitions above, the model of real-world traffic network can be given in the following.

Let digraph $D = (V, A)$ represent the road network. In the digraph V and A represent the set of junctions and roads, respectively. Then the digraph D is strongly connected and has no loops and parallel arcs. Notice that the roundabout is

treated as a junction since it has no functional difference in our location problem.

Let digraph $L = (V, A)$ represent the traffic constraints. In L , V represents the set of roads. A represents the set of turn limitations, respectively. The arc joining one road to another exists at the presence of turn limitation at the junction. Then the digraph L does not have any loops and parallel arcs, and is a subdigraph of D^* .

Let hypergraph $C = (X, \mathcal{F})$ represent the traffic cycles. X of the hypergraph C represents the set of roads. \mathcal{F} represents the set of road-sets. $F_i \in \mathcal{F}$ is the arc-set of a directed cycle in the road network D .

Let hypergraph $I = (X, \mathcal{F})$ represent the traffic circuits. X represents the set of roads. \mathcal{F} represents the set of road-sets. $F_i \in \mathcal{F}$ is the arc-set of a directed circuit in D . The traffic circuit indicates a closed route in which each road is passed only once. The traffic cycle is similar where the junctions are passed only once. The two definitions are analogous to the directed cycle and directed circuit in the digraph, as the simplifications of the real-world road network.

Let hypergraph $I_\epsilon = (X, \mathcal{F}_\epsilon)$, where $\mathcal{F}_\epsilon = \{F_i : |F_i| > \epsilon; F_i \in \mathcal{F}\}$ represent the traffic circuits with length longer than ϵ .

In our model, we also make the assumption that short traffic circuits are not essential and thus ignored.

C. Problem Statement

Our goal is to measure emissions of all on-road vehicles. This is achieved by locating traffic emission monitors on the road network. There is no doubt that the amount and location of the monitors have a significant influence on the monitoring performance. Since the amount of monitors is constrained by the economic considerations, the optimal location of the monitors thus becomes one key technique in the vehicle emission RSS.

Based on the graph theory description, our location problem is to find the minimum set of arcs on which traffic emission monitors are located, in order to capture as many on-road vehicles as possible. We make an assumption that the traffic flow has the symmetric property, which means that all on-road vehicles will eventually pass through a circuit. It needs to be noticed that this paper ignores the circuits whose length is smaller than 3. In other words, if every traffic circuit of the road network contains at least one road that is located with a monitor, every on-road vehicle can be measured at least for once. Therefore, the problem, aimed at capturing all in-use vehicles in the traffic network, can be formulated as to find a minimum set of arcs that intersects every circuit, and immediately is transformed into finding the minimum transversal of $I = (X, \mathcal{F})$ where $X(I) = A(D)$, and consequently the minimum transversal of $I_\epsilon = (X, \mathcal{F}_\epsilon)$.

III. LOCATION STRATEGY

The location strategy is composed of two steps. In the first step, the algorithm to find all the directed circuits according to the depth first searching process is developed to obtain hypergraph-based set of directed circuits. In the second step,

Algorithm 1 DICYCFIND

Input: A strongly connected digraph $D = (V, A)$

Initialize: A stack $P := \emptyset$, two sets $Q := \emptyset$ and $S := \emptyset$, two integers $\ell := 1$ and $t := 0$

Output: A set of directed cycles $C = (X, \mathcal{F})$

```

1: for  $i = 1$  to  $|V| - 1$  do
2:   increase  $t$  by 1
3:   push  $v_i$  into  $P$ 
4:   while 1 do
5:     set  $S := N^+(v)$  where  $v = P(t)$ 
6:     set  $S := S - \{v_j : j \leq i\}$ 
7:     set  $S := S - \{v : v \in P\}$ 
8:     set  $S := S - \{v : \vec{uv} \in Q\}$  where  $u = P(t)$ 
9:     if  $S = \emptyset$  then
10:      if  $P(t) = v_i$  then
11:        break the circulation
12:      end if
13:      if  $\vec{uv}_i \in A$  where  $u = P(t)$  then
14:        set  $F_\ell := A(P)$ 
15:        increment  $\ell$  by 1
16:      end if
17:      pop  $P$ 
18:      decrease  $t$  by 1
19:    else
20:      push  $S(1)$  into  $P$ 
21:      increase  $t$  by 1
22:      add  $\vec{uv}$  into  $Q$  where  $u = P(t - 1)$  and  $v = P(t)$ 
23:      delete  $\vec{uv}$  from  $Q$  where  $u = P(t)$  and  $v \in V$ 
24:    end if
25:  end while
26: end for
27: set  $X := A$ 
28: set  $\mathcal{F} = \{F_1, F_2, \dots\}$ 
29: return  $C = (X, \mathcal{F})$ 

```

an approximation algorithm to find the greedy transversal is designed in order to determine the roads to set monitors.

A. Step 1: Finding Circuits

It is known that the line digraph is strongly connected if and only if the digraph is strongly connected [48]. Thus, finding all the circuits in a digraph is equivalent to finding all the directed cycles in its line digraph. Consequently, the turn constraints can be easily dealt with by making an operation of $D^* - L$ equal to $(V, A(D^*) - A(L))$. Therefore, we can focus only on finding all the directed cycles of $D^* - L$. The directed cycles finding algorithm (DICYCFIND, Algorithm 1) is designed for this purpose.

The algorithm works as follows. $D = (V, A)$ is a strongly connected digraph, that has no vertex with zero in-degree or out-degree. Arrange the vertex set V as $1, 2, \dots, |V|$, and start from v_1 to extend directed path $P = (v_1, v_2, \dots, v_k)$ until there is no other vertex reachable from v_k . Then we check whether there exists an arc $\vec{v_k v_1}$, if so, we can obtain a directed cycle $C = (v_1, v_2, \dots, v_k)$ at this step. Otherwise, according to the depth first principle we need return to v_{k-1} and search

whether there exists an arc from v_{k-1} to another vertex v_i , $v_i \notin \{v_1, v_2, \dots, v_k\}$, if so, we can extend this directed path to v_i , otherwise, we should back to v_{k-2} and repeat the operation until it returns to v_1 . At this point, all directed paths starting from v_1 have been found and also the corresponding directed cycles. After the searching from v_1 is completed, repeat the procedure from next vertex. With all vertices searched, we can obtain all directed cycles in the digraph. It is worth noting that in order to avoid that the directed cycle containing q vertices is generated for q times, namely, that the same directed cycle is obtained when searching from every vertex on the cycle, let v_i be the original vertex, and then when searching from v_i , we need not to visit the vertex v_j where $j \leq i$. That is to say, the original vertex of directed cycle should be with the smallest subscript.

The DICYCFIND algorithm is developed according to the extending and shrinking of the directed path, and the stack with the last-in-first-out principle is suitable for describing this procedure. Let P and t represent the stack and its top, respectively. S contains the vertices that can next be visited. $S = \emptyset$ means that the directed path cannot be extended any more, then a judgement should be conducted whether a directed cycle can be obtained, as shown in statements 13–15. Otherwise, extend the directed path and record the vertices that has been visited, as shown in statements 20–23. A complete depth-first-searching process ends until the directed path back to the origin, as shown in statements 10 and 11. The similar searching should be conducted for $|V| - 1$ times to find all directed cycles. This algorithm will extend the directed path as long as possible, and attempt to search another branch at every vertex when the extending cannot be continued. Hence, it is able to find all the directed paths from the origin to arbitrary another vertex, thus all the directed cycles can be found.

There is a double-layer circulation in the algorithm and the times of the inner circulation is difficult to determine. The experience tell us that every vertex has a nearly equal out-degree in the road network, so the times can be approximately treated as $(d + 1)i$, where d is the average out-degree and i is the current amount of vertices by the external circulation. The constant 1 is caused by the judgement if backtrack or not. Therefore, the sum of circulation times is $\sum_{i=1}^{|V|-1} (d + 1)i$. It is noted that the average degree d is much smaller than the digraph's order $|V|$, except in the complete digraph where d equals $|V| - 1$. As to the road network, the computational complexity of DICYCFIND algorithm is $\mathcal{O}(|V|^2)$.

B. Step 2: Finding Transversal

Using the DICYCFIND algorithm a hypergraph-based set of circuits is obtained and the second step is to find its transversal as small as possible. We first simplify the hypergraph, as shown in the HYPERSIM algorithm.

In the HYPERSIM algorithm (Algorithm 2), statements 1, 2, 8, and 9 constitute a double-layer circulation with times of

$$\sum_{i=1}^{|\mathcal{F}|-1} |\mathcal{F}| - i = \frac{|\mathcal{F}|(|\mathcal{F}| - 1)}{2} = \frac{|\mathcal{F}|^2}{2} - \frac{|\mathcal{F}|}{2}$$

Algorithm 2 Hypergraph Simplification (HYPERSIM)

Input: A hypergraph $H = (X, \mathcal{F})$

Initialize: A set $\mathcal{F}' := \mathcal{F}$

Output: A simple hypergraph $H' = (X, \mathcal{F}')$

```

1: for  $i = 1$  to  $|\mathcal{F}| - 1$  do
2:   for  $j = i + 1$  to  $|\mathcal{F}|$  do
3:     if  $F_i \subseteq F_j$  then
4:       set  $\mathcal{F}' := \mathcal{F}' - \{F_j\}$ 
5:     else if  $F_i \supseteq F_j$  then
6:       set  $\mathcal{F}' := \mathcal{F}' - \{F_i\}$ 
7:     end if
8:   end for
9: end for
10: return  $H' = (X, \mathcal{F}')$ 

```

Algorithm 3 Greedy Transversal Finding (GRTRANSFIND)

Input: A simple hypergraph $H = (X, \mathcal{F})$

Initialize: A hypergraph $S_1 := H$, a set $T := \emptyset$, an integer $i := 1$

Output: A transversal T of H

```

1: delete all the isolated vertices
2: while  $S_i \neq \emptyset$  do
3:   create  $t_i := \emptyset$ 
4:   for  $k = 1$  to  $|X(S_i)|$  do
5:     if  $d(t_i) < d(x_k)$  where  $x_k \in X(S_i)$  then
6:       set  $t_i := x_k$ 
7:     end if
8:   end for
9:   add  $t_i$  into  $T$ 
10:  increase  $i$  by 1
11:  set  $S_i := S_{i-1} - S_{i-1}(t_{i-1})$ 
12: end while
13: return  $T$ 

```

which essentially generate a series of pairwise combination in \mathcal{F} with the cardinality of $\binom{|\mathcal{F}|}{2}$, comparing these pairs to eliminate repeated hyperedges. These operations cause the primary computation resulting in the computational complexity of $\mathcal{O}(|\mathcal{F}|^2)$. Statements 3–9 attempt to find whether a pair exists where an element contains another or not, if so the superset will be deleted from \mathcal{F}' . At the end of the algorithm it will return a simple hypergraph and the correctness is self-evident. Specially it is noted that the operation is not conducted in the set \mathcal{F} but \mathcal{F}' instead for not to change the values of input.

The next work is to find a minimum transversal of the simplified hypergraph by the HYPERSIM algorithm, which is, however, a nondeterministic polynomial complete problem. We here treat it by approximations based on the greedy strategy which selects the best current option at each step only.

In the GRTRANSFIND algorithm (Algorithm 3), statement 3 creates an empty vertex t_i at the beginning of every circulation in order to record the selected vertex. By deleting the star of the selected vertex $S_i(x_i)$ at the end of every circulation, a transversal can be generated until the hypergraph S_i is empty.

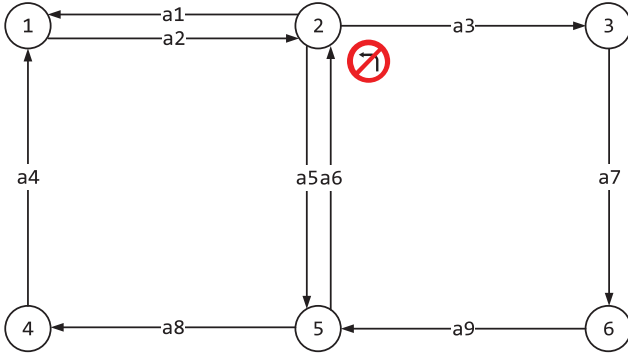


Fig. 3. Diagram of a digraph with turn constraint. The digraph has six vertices and nine arcs. There exists a turn limitation from a_6 to a_1 .

The principle of selecting vertex in every circulation is to choose the vertex with the largest degree as shown in statements 3–7. Considering the worst situation that every vertex intersects only one hyperedge, the external circulation will be conducted for $|V|$ times and the inner $|V| - i$ times. So the sum is

$$\sum_{i=1}^{|V|} |V| - i = \frac{|V|(|V| - 1)}{2} = \frac{|V|^2}{2} - \frac{|V|}{2}.$$

Therefore, this is a polynomial-time algorithm with computational complexity of $\mathcal{O}(|V|^2)$ which is available in the large-scale situation. The GRTRANSFIND algorithm will output a transversal with the ratio of $1 + \log \Delta$ whose proof will be seen in the Appendix.

IV. ILLUSTRATIVE EXAMPLES

A. Test 1: Simulation

Consider a digraph with certain turn constraints as shown in Fig. 3. The digraph D has the following nine directed circuits:

- $J_1 = \{v_1, a_2, v_2, a_1, v_1\}$
- $J_2 = \{v_2, a_5, v_5, a_6, v_2\}$
- $J_3 = \{v_1, a_2, v_2, a_5, v_5, a_6, v_2, a_1, v_1\}$
- $J_4 = \{v_1, a_2, v_2, a_5, v_5, a_8, v_4, a_4, v_1\}$
- $J_5 = \{v_2, a_3, v_3, a_7, v_6, a_9, v_5, a_6, v_2\}$
- $J_6 = \{v_2, a_1, v_1, a_2, v_2, a_3, v_3, a_7, v_6, a_9, v_5, a_6, v_2\}$
- $J_7 = \{v_1, a_2, v_2, a_3, v_3, a_7, v_6, a_9, v_5, a_8, v_4, a_4, v_1\}$
- $J_8 = \{v_1, a_2, v_2, a_3, v_3, a_7, v_6, a_9, v_5, a_6, v_2, a_5, v_5, a_8, v_4, a_4, v_1\}$
- $J_9 = \{v_1, a_2, v_2, a_5, v_5, a_6, v_2, a_3, v_3, a_7, v_6, a_9, v_5, a_8, v_4, a_4, v_1\}$.

Vehicles on a_6 cannot turn to a_1 at the junction v_2 . Hence J_3 and J_6 should be dropped.

As mentioned earlier, the digraph-based road network D should be transformed into its line digraph D^* as shown in Fig. 4. The red dashed arc coupled with the vertices a_1 and a_6 constitute the turn constraints L . Applying the DICYCFIND algorithm to the remainder of the graph without the arc $\overrightarrow{a_6 a_1}$, i.e., $D^* - L$, it generates all the directed circuits of D eliminating the affect of turn constraints. As shown in Fig. 5,

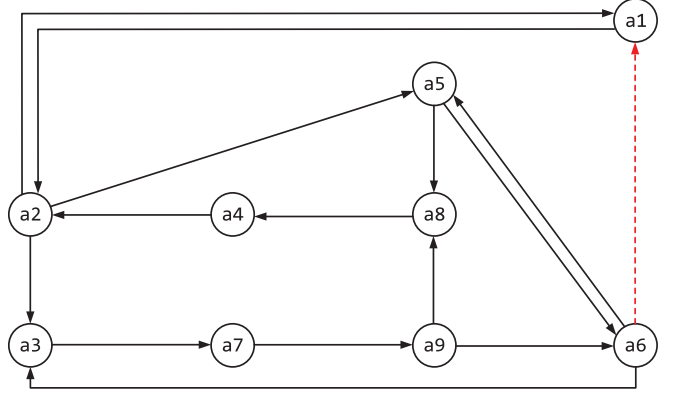


Fig. 4. Diagram of line digraph. The turn constraint in Fig. 3 leads to the deletion of arc $a_6 a_1$, which is represented by the red dashed line.

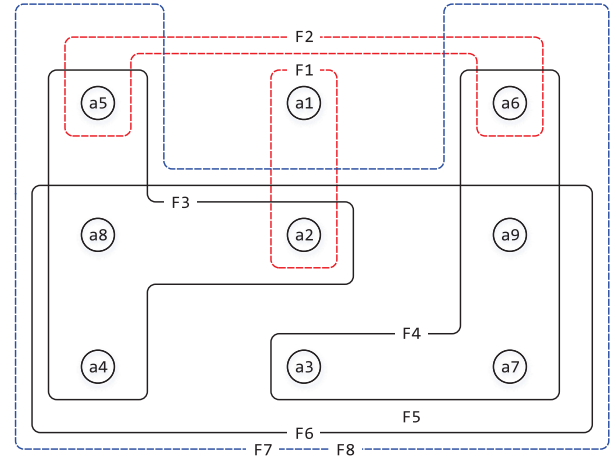


Fig. 5. Diagram of hypergraph-based directed circuits set. The red dashed lines represent circuits whose cardinality is equal to 2. The blue dashed line represents two circuits with the same set of arcs.

the set of directed circuits $I = (X, \mathcal{F})$ is composed of $X = \{a_i : i = 1, 2, \dots, 9\}$ and $\mathcal{F} = \{F_i : i = 1, 2, \dots, 7\}$, where

- $F_1 = \{a_1, a_2\}$
- $F_2 = \{a_5, a_6\}$
- $F_3 = \{a_2, a_5, a_8, a_4\}$
- $F_4 = \{a_3, a_7, a_9, a_6\}$
- $F_5 = \{a_2, a_3, a_7, a_9, a_8, a_4\}$
- $F_6 = \{a_2, a_3, a_7, a_9, a_6, a_5, a_8, a_4\}$
- $F_7 = \{a_2, a_5, a_6, a_3, a_7, a_9, a_8, a_4\}$.

Deleting the directed circuits with small cardinality not more than 2 (the red dashed hyperedge), it is obtained $I_2 = (X, \mathcal{F}_2)$, where $\mathcal{F}_2 = \mathcal{F} - \{F_1, F_2\}$. By applying the HYPERSIM algorithm the simplified hypergraph $I'_2 = (X, \mathcal{F}'_2)$ is obtained, where $\mathcal{F}'_2 = \mathcal{F}_2 - \{F_6, F_7\}$ as the rest partial hypergraph with deleting the red and blue dashed hyperedges. The set $T = \{a_2, a_3\}$ is one of the transversals of I'_2 . By locating the traffic emission monitors on the two roads,

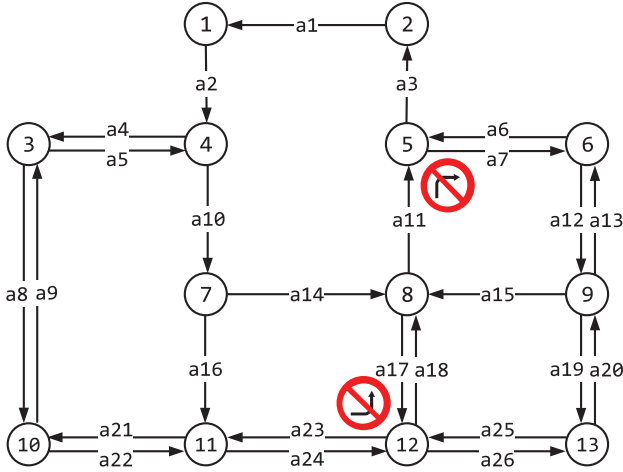


Fig. 6. Diagram of real-world road network. This digraph is from [29], and two turn constraints are set on it.

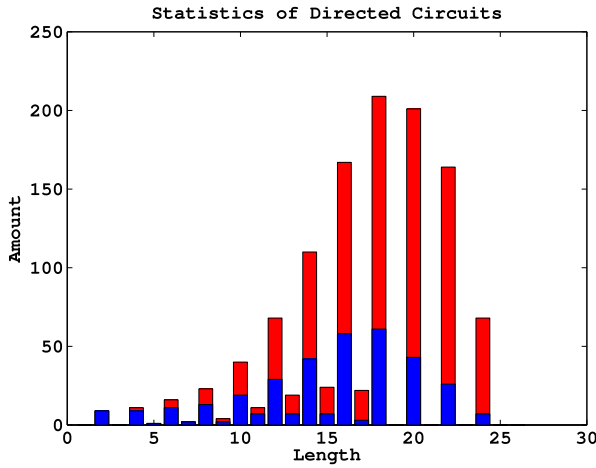


Fig. 7. Statistics of directed circuits. Without the turn constraints, the distribution of number of directed circuits with different length is shown as the red bars. After deleting circuits that do not exist due to the turn constraints, the distribution is shown in blue ones.

all the traffic circuits with length longer than 2 are under monitoring.

B. Test 2: First Real-World Test

We consider a practical road network modeled as a digraph with 13 vertices and 26 arcs as shown in Fig. 6.

In Fig. 7, it shows that without considering the turn constraints, 1169 directed circuits are found and its distribution according to length is illustrated by the red bars. It reveals that there are only a few directed circuits with odd length. The amount peaks at the length equalling 18, which may be treated as a feature of the road network to describe its complexity or traffic capacity. By eliminating the turn constraints, the sum amount of the directed circuits reduce sharply to 356, indicating its great affect on the traffic capacity.

The notations in Table I are as follows. \mathcal{I} , I , and I_ϵ represent the set of directed circuits of the road network without

TABLE I
STATISTICS OF RESULTS OF PROPOSED LOCATION STRATEGY

	$ \mathcal{F} $	$ \mathcal{F}' $	Δ	τ	τ^\dagger	$\frac{\tau}{\tau^\dagger}$	$\frac{\tau}{ X }$
\mathcal{I}	1169	23	8	10	9	1.11	0.38
I	356	18	7	10	8	1.25	0.38
I_2	347	19	11	5	4	1.25	0.19
I_4	338	20	14	4	3	1.33	0.15
I_6	326	23	18	3	2	1.5	0.12
I_8	311	25	23	2	2	1	0.08
I_{10}	290	36	34	2	2	1	0.08
I_{12}	254	49	47	2	2	1	0.08
I_{14}	205	56	55	2	2	1	0.08
I_{16}	140	40	40	1	1	1	0.04
I_{18}	76	23	23	1	1	1	0.04
I_{20}	33	9	9	1	1	1	0.04
I_{22}	7	1	1	1	1	1	0.04

considering its turn constraints, with these constraints and those circuits with length smaller than ϵ being deleted. Since there are few odd directed circuits, the even, say I_2 , are selected to do the experiment. The symbols $|\mathcal{F}|$ and $|\mathcal{F}'|$ represent the amount of directed circuits and its simplified situation, respectively. Δ , τ , and τ^\dagger represent the maximum degree, greedy transversal number, and minimum transversal number, respectively. $(\tau/|X|)$ is referred to as the location-ratio, in a way to estimate the programme cost.

- 1) The sudden change in the variation of $|\mathcal{F}|$ indicates that the turn constraints have a great affect to the amount of directed circuits.
- 2) $|\mathcal{F}'|$ does not decrease with the decreasing of $|\mathcal{F}|$, showing that some directed circuits with larger length is composed of the same smaller ones. So the $|\mathcal{F}'|$ peaks at I_{14} instead of decreasing.
- 3) $|\mathcal{F}'|$ of \mathcal{I} is equal to the amount of directed cycles of the original digraph for the reason that every directed circuit contains at least one directed cycle in its sequence.
- 4) Generally speaking $|\mathcal{F}'|$ is much smaller than $|\mathcal{F}|$, so it is deduced that the small directed circuits can be treated as the cores of road network.
- 5) The transversal generated by the GRTRANSFIND algorithm approximates the minimum transversal with a extremely small error for small Δ .
- 6) With ϵ increasing, smaller directed circuits are deleted and the difference between $|\mathcal{F}'|$ and Δ is getting smaller even eliminated, such that to reduce the location-ratio, namely, the sum cost of the vehicle emission RSS.
- 7) The determination of ϵ is based on the financial budget or the statistics on the vehicles' traveling routes.

C. Test 3: Second Real-World Test

This example considers the road network shown in Fig. 8. Table II shows nine comparison experiments and their results. The amount of monitors are set as 3, 10, and 20, respectively. The experience-based method has two steps: one is to divide the road network equally into several areas within which the amount is equal to that of the monitors, and then select a road with highest traffic flow for each area. In fact, placing devices

TABLE II
COMPARISON RESULTS

Experiment		number of entries	number of vehicles	average degree
3 monitors	Located by proposed algorithm	141121	58989	0.418
	Located by experience	158187	61851	0.391
	Located randomly	90853	31980	0.352
10 monitors	Located by proposed algorithm	436195	151793	0.348
	Located by experience	420194	94543	0.225
	Located randomly	274881	51403	0.187
20 monitors	Located by proposed algorithm	752643	245362	0.326
	Located by experience	819697	176235	0.215
	Located randomly	670408	172295	0.257



Fig. 8. Satellite aerial photography of tested area around the University of Science and Technology of China that is located in Anhui, China (from BaiduMap). The lines in the photo stand for the roads, and the orange one represents a viaduct. The network can be modeled as a digraph with 34 vertices and 108 arcs.

randomly onto the road network is also a frequently-used method. In all the experiments, we use a transportable platform to carry each license recognizer to the location rather than truly installing the traffic emission monitors. After all the recognizers are set to their location and the operational parameters are well adjusted, the license recognizers started up 24 h measurement persisting for a week.

The information of interest include the number of entries, the number of vehicles and the average degree. The *number of entries* is used to describe the sample scale, increasing by one with a vehicle driving through a license recognizer. It is noteworthy that the number of entries obtained in our experiments is much larger than that of installing the vehicle emission monitors for the emissions from different vehicles may not be detected when the vehicles pass through the monitor in parallel. The *average degree* is the ratio of the number of vehicles to that of entries, which is supposed to be large since it reveals that the multiplicity of measuring is higher with the average degree getting smaller. Larger average degree means superior allocation of monitors.

As shown in Table II, with the number of monitors increasing, the number of entries and the number of vehicles both rise obviously. Locating randomly gets the smallest number of entries in all three experiments, while when it comes to 20 monitors, the disparity between locating randomly and any another scheme is not that noticeable. Combining the number of entries and number of vehicles, although the scheme locating by experience tends to achieve more entries than locating by the proposed algorithm, the number of different vehicles in the scheme of locating by experience has an opposite tendency. The average degree of locating by the proposed algorithm is larger than that of locating by experience or locating randomly in all three situations. With the number of located monitors increasing, more vehicles can be captured, while the average degree gradually decreases. It shows that the scheme of locating monitors by experience has the same downtrend. It should be noticed that the scheme of locating randomly is a little different from the two schemes above. In the experiment of 20 monitors, locating randomly gets an average degree of 0.257, which is larger than the value 0.187 in the situation of ten monitors, and this value is even larger than locating by experience. The proposed strategy always has larger average degree than any another scheme which can be found in the table. Locating by experience gets larger average degree than locating randomly when the number of monitors is 3 or 10, and in the last situation, this relation is opposite. From the analysis above, we can conclude that the proposed location strategy can perform better than the common location methods in practical application.

The proportion of amount of cars detected by monitors of the same amount, over all the vehicles can be detected for more than one time. In Fig. 9, the inner, middle, and external circles represent results of the situations locating by proposed algorithm, locating by experience, and locating randomly, respectively. We can find that the vehicles detected by only one monitor have taken up the majority and the proportions of the three situations have slight differences. This may be due to that the amount of monitors is too small to cover such a wide road network. Locating three monitors to the main

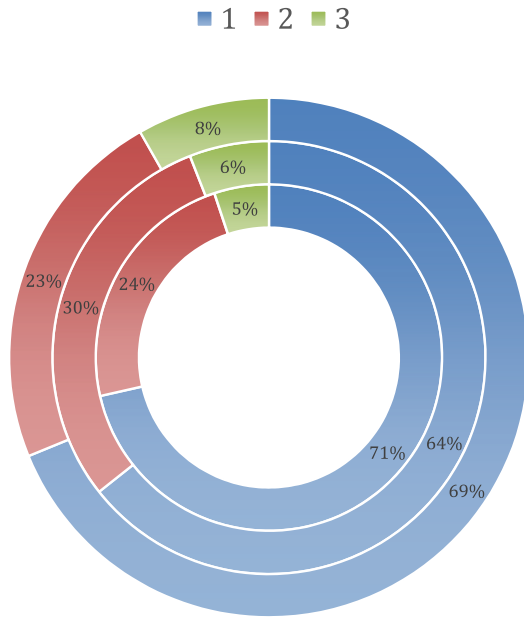


Fig. 9. Pie graph of cars detected by different amount monitors in the three-monitor case. The blue part represents the proportion of number of vehicles that are captured by only one monitor, and the red part for the proportion that are captured by two monitors, the green part for the proportion that are captured by all three monitors. Figs. 10 and 11 have the similar meaning.

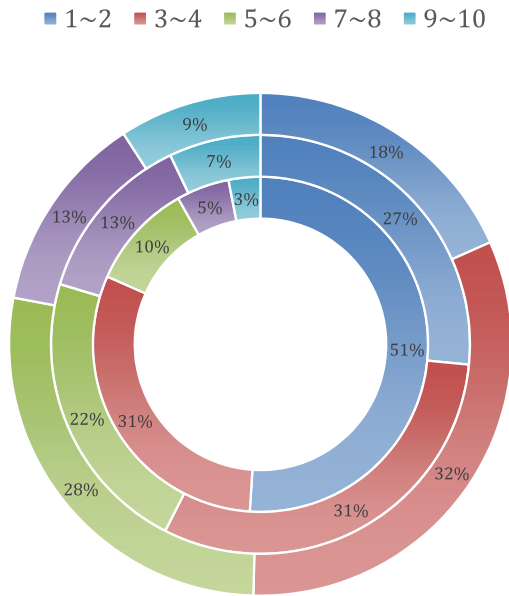


Fig. 10. Pie graph of cars detected by different amount monitors in the ten-monitor case.

roads in different area is enough to reduce the multiplicity. However, to the ten-monitor case as shown in Fig. 10, the results are totally different from that of three-monitor case. It is deduced that most of the vehicles are detected by one to four monitors while using the proposed location strategy, and even over half of the cars can be detected for less or equal to twice which can reduce the multiplicity to a great extent. The results of locating by experience or randomly show that it still has a lot of vehicles that are detected by six monitors which is a waste of resource caused by unreasonable location.

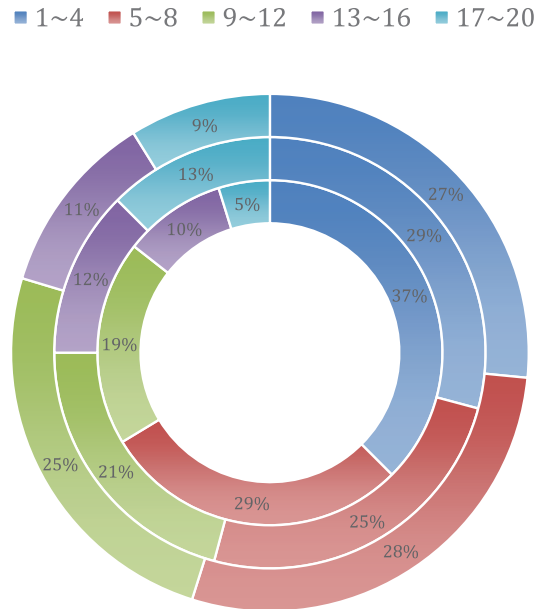


Fig. 11. Pie graph of cars detected by different amount monitors in the 20-monitor case.

In the 20-monitor case with its results shown in Fig. 11, the performance of the proposed algorithm is not more brilliant than that of locating monitors by experience or randomly compared to the ten-monitor case. This can be interpreted as that if there are too many monitors, even meeting the condition that every road can be allocated one monitor, it is not necessary to develop such a location strategy. In conclusion, the proposed location strategy is essentially to average the monitors to avoid the multidetection as much as possible, hence achieving the highest average degree. The experience-based location strategy has ignored the fact that people are more likely to drive their vehicles along main roads so that it will raise the occurrence of multidetection.

V. CONCLUSION

We formulate a novel location problem in smart transportation where the minimum subset of roads on which traffic emission monitors are placed is to be found. Since it is intractable to quantify the influencing factors such as geographic position and congestion situation, and information like traffic flow of the whole road network is not easily accessible even for the national traffic administrative department, in this paper we solve this problem only using the topological structure and some other available information of the traffic network. We propose a two-step location strategy using both depth first searching and greedy strategy to find the minimum set of roads with traffic emission monitors, based on the digraph modeled from the traffic network, whose performance is validated by both theoretical proof and illustrative examples. Future works may focus on the inclusion of the device failure probability and other practical implementation issues.

APPENDIX

Theorem 1: The GRTRANSFIND algorithm will output a transversal with the ratio of $1 + \log \Delta$.

Proof: First, statement 10 can be written as

$$\begin{aligned} S_1 &= H \\ S_2 &= S_1 - S_1(t_1) \\ S_3 &= S_2 - S_2(t_2) \\ &\vdots \\ \emptyset &= S_\tau - S_\tau(t_\tau) \end{aligned}$$

where $\tau = |T|$, and then

$$\begin{aligned} H &= S_1 \\ S_1(t_1) &= S_1 - S_2 \\ S_2(t_2) &= S_2 - S_3 \\ &\vdots \\ S_\tau(t_\tau) &= S_\tau - \emptyset \end{aligned}$$

and then $\bigcup_{i=1}^\tau S_i(t_i) = H$. For $S_i(t_i) \subset S(t_i)$ such that $H = \bigcup_{i=1}^\tau S_i(t_i) \subseteq \bigcup_{i=1}^\tau S(t_i) \subseteq H$, resulting in $\bigcup_{i=1}^\tau S(t_i) = H$ that every hyperedge in H can be traversed by the vertices in T . This proves the correctness of the GRTRANSFIND algorithm.

Let τ^\dagger denote the cardinality of the minimum transversal and ℓ_λ the times selecting the vertex with the degree of λ . We have

$$\tau = |T| = \ell_1 + \ell_2 + \cdots + \ell_{\lambda+1} + \cdots + \ell_\Delta$$

where Δ is the maximum degree of H . By denoting $\ell_\Delta + \ell_{\Delta-1} + \cdots + \ell_{\lambda+1} = k$, the partial hypergraph S_{k+1} is obtained at the end of the $k + 1$ th circulation. Then

$$\lambda \ell_\lambda + (\lambda - 1)\ell_{\lambda-1} + \cdots + 2\ell_2 + \ell_1 = |\mathcal{F}(S_{k+1})| \leq \lambda \tau^\dagger$$

then

$$\left(\frac{1}{\lambda} - \frac{1}{\lambda + 1}\right)(\ell_1 + 2\ell_2 + \cdots + \lambda \ell_\lambda) \leq \frac{1}{\lambda + 1} \tau^\dagger$$

then

$$\begin{aligned} \left(1 - \frac{1}{2}\right)\ell_1 &\leq \frac{1}{2} \tau^\dagger \\ \left(\frac{1}{2} - \frac{1}{3}\right)(\ell_1 + 2\ell_2) &\leq \frac{1}{3} \tau^\dagger \\ \left(\frac{1}{3} - \frac{1}{4}\right)(\ell_1 + 2\ell_2 + 3\ell_3) &\leq \frac{1}{4} \tau^\dagger \\ &\vdots \\ \left(\frac{1}{\Delta - 1} - \frac{1}{\Delta}\right)(\ell_1 + 2\ell_2 + \cdots + (\Delta - 1)\ell_{\Delta-1}) &\leq \frac{1}{\Delta} \tau^\dagger \\ \frac{1}{\Delta}(\ell_1 + 2\ell_2 + \cdots + \Delta \ell_\Delta) &\leq \tau^\dagger. \end{aligned}$$

Summing each side of the inequations above yields

$$\tau = \sum_{\lambda=1}^{\Delta} \ell_\lambda \leq \left(1 + \frac{1}{2} + \cdots + \frac{1}{\Delta}\right) \leq (1 + \log \Delta) \tau^\dagger$$

and therefore it is a $(1 + \log \Delta)$ -approximation algorithm. Obviously the ratio $\mathcal{O}(\log \Delta)$ at Δ trends to a very large number. ■

REFERENCES

- [1] L. Bayer-Oglesby *et al.*, "Living near main streets and respiratory symptoms in adults: The Swiss Cohort study on air pollution and lung diseases in adults," *Amer. J. Epidemiol.*, vol. 164, no. 12, pp. 1190–1198, Oct. 2006.
- [2] A. J. Venn, S. A. Lewis, M. Cooper, R. Hubbard, and J. Britton, "Living near a main road and the risk of wheezing illness in children," *Amer. J. Respiratory Crit. Care Med.*, vol. 164, no. 12, pp. 2177–2180, Dec. 2006.
- [3] A. Baccarelli *et al.*, "Living near major traffic roads and risk of deep vein thrombosis," *Circulation*, vol. 119, no. 24, pp. 3118–3124, Jun. 2009.
- [4] P. Matjaž and A. Szolnoki, "Coevolutionary games—A mini review," *Bio Syst.*, vol. 99, no. 2, pp. 109–125, 2009.
- [5] D. Helbing *et al.*, "Saving human lives: What complexity science and information systems can contribute," *J. Stat. Phys.*, vol. 158, no. 3, pp. 735–781, 2014.
- [6] M. R. D'Orsogna and M. Perc, "Physics for better human societies: Reply to comments on 'statistical physics of crime: A review,'" *Phys. Life Rev.*, vol. 12, pp. 40–43, Mar. 2015.
- [7] Ministry of Environment Protection of the Peoples Republic of China, "China vehicle emission control annual report: 2015 (in Chinese)," Jan. 2016.
- [8] G. A. Bishop, J. R. Starkey, A. Ihlenfeldt, W. J. Williams, and D. H. Stedman, "IR long-path photometry: A remote sensing tool for automobile emissions," *Anal. Chem.*, vol. 61, no. 10, pp. 671A–677A, 1989.
- [9] Y. Zhang, D. H. Stedman, G. A. Bishop, P. L. Guenther, and S. P. Beaton, "Worldwide on-road vehicle exhaust emissions study by remote sensing," *Environ. Sci. Technol.*, vol. 29, no. 9, pp. 2286–2294, 1995.
- [10] G. A. Bishop and D. H. Stedman, "Measuring the emissions of passing cars," *Accounts Chem. Res.*, vol. 29, no. 10, pp. 489–495, 1996.
- [11] E. Castillo, Z. Grande, A. Calviño, W. Y. Szeto, and H. K. Lo, "A state-of-the-art review of the sensor location, flow observability, estimation, and prediction problems in traffic networks," *J. Sensors*, vol. 2015, 2015, Art. no. 903563.
- [12] E. Castillo, J. M. Menéndez, and P. Jiménez, "Trip matrix and path flow reconstruction and estimation based on plate scanning and link observations," *Transp. Res. B Methodol.*, vol. 42, no. 5, pp. 455–481, May 2008.
- [13] M. Gentili, "New models and algorithms for the location of sensors on traffic networks," Ph.D. dissertation, Dept. Stat., Univ. Rome, Rome, Italy, 2002.
- [14] M. Gentili and P. B. Mirchandani, "Locating active sensors on traffic networks," *Annal. Oper. Res.*, vol. 136, no. 1, pp. 229–257, Jan. 2005.
- [15] M. Gentili and P. B. Mirchandani, "Locating sensors on traffic networks: Models, challenges and research opportunities," *Transp. Res. C Emerg. Technol.*, vol. 24, pp. 227–255, Sep. 2012.
- [16] W. H. K. Lam and H. P. Lo, "Accuracy of O/D estimates from traffic counts," *Traffic Eng. Control*, vol. 31, no. 6, pp. 358–367, 1990.
- [17] A. Ehler, M. G. H. Bell, and S. Grosso, "The optimisation of traffic count locations in road networks," *Transp. Res. B Methodol.*, vol. 40, no. 6, pp. 460–479, Jun. 2006.
- [18] H. Yang and J. Zhou, "Optimal traffic counting locations for origin–destination matrix estimation," *Transp. Res. B Methodol.*, vol. 32, no. 2, pp. 109–126, Feb. 1998.
- [19] H. Yang, C. Yang, and L. Gan, "Models and algorithms for the screen line-based traffic-counting location problems," *Comput. Oper. Res.*, vol. 33, no. 3, pp. 836–858, Mar. 2006.
- [20] L. Bianco, G. Confessore, and P. Reverberi, "A network based model for traffic sensor location with implications on O/D matrix estimates," *Transp. Sci.*, vol. 35, no. 1, pp. 50–60, Jan. 2001.
- [21] L. Bianco, G. Confessore, and M. Gentili, "Combinatorial aspects of the sensor location problem," *Annal. Oper. Res.*, vol. 144, no. 1, pp. 201–234, 2006.
- [22] L. Gan, H. Yang, and S. C. Wong, "Traffic counting location and error bound in origin–destination matrix estimation problems," *J. Transp. Eng.*, vol. 131, no. 7, pp. 524–534, Jul. 2005.
- [23] L. Gan and H. Yang, "Integer programming models for optimal selection of screen lines in road networks," in *Proc. Transp. Plan. Manag. 21st Century*, Hong Kong, 2001, pp. 122–130.
- [24] S.-R. Hu, S. Peeta, and C.-H. Chu, "Identification of vehicle sensor locations for link-based network traffic applications," *Transp. Res. B Methodol.*, vol. 43, nos. 8–9, pp. 873–894, Sep. 2009.
- [25] M. Ng, "Synergistic sensor location for link flow inference without path enumeration: A node-based approach," *Transport. Res. B Methodol.*, vol. 46, no. 6, pp. 781–788, Jul. 2012.

- [26] L. Bianco, C. Cerrone, R. Cerulli, and M. Gentili, "Locating sensors to observe network arc flows: Exact and heuristic approaches," *Comput. Oper. Res.*, vol. 46, pp. 12–22, Jun. 2014.
- [27] W. Gu, D. F. Hsu, and X. Jia, "On a network sensing problem," *J. Interconnect. Netw.*, vol. 7, no. 1, pp. 63–73, Mar. 2006.
- [28] W. Gu and X. Jia, "On a traffic control problem," in *Proc. 8th Int. Symp. Parallel Architect. Algorithms Netw.*, Las Vegas, NV, USA, 2005, p. 6.
- [29] P.-Q. Lin and J.-M. Xu, "Layout of traffic detectors in road network based on graph theory," *Control Theory Appl.*, vol. 27, no. 12, pp. 1605–1611, Dec. 2010.
- [30] L. Yan, "On the traffic flow control system," HKU thesis, Dept. Comput. Sci., Univ. Hong Kong, Hong Kong, 2001.
- [31] F. Chin, M. Chrobak, and L. Yan, "Algorithms for placing monitors in a flow network," *Algorithmica*, vol. 68, no. 1, pp. 1–15, Jan. 2014.
- [32] D. R. Morrison and S. E. Martonosi, "Characteristics of optimal solutions to the sensor location problem," *Annal. Oper. Res.*, vol. 226, no. 1, pp. 463–478, Jan. 2015.
- [33] H. M. La, W. H. Sheng, and J. M. Chen, "Cooperative and active sensing in mobile sensor networks for scalar field mapping," *IEEE Trans. Syst., Man, Cybern., Syst.*, vol. 45, no. 1, pp. 1–12, Jan. 2015.
- [34] R. Li and L. Jia, "On the layout of fixed urban traffic detectors: An application study," *IEEE Intell. Transp. Syst. Mag.*, vol. 1, no. 2, pp. 6–12, Sep. 2009.
- [35] X. Li and Y. Ouyang, "Reliable sensor deployment for network traffic surveillance," *Transp. Res. B Methodol.*, vol. 45, no. 1, pp. 218–231, Jan. 2011.
- [36] L. Zhen, K. Wang, and H.-C. Liu, "Disaster relief facility network design in metropolises," *IEEE Trans. Syst., Man, Cybern., Syst.*, vol. 45, no. 5, pp. 751–761, May 2015.
- [37] L. Zhen, W. Wang, and D. Zhuge, "Optimizing locations and scales of distribution centers under uncertainty," *IEEE Trans. Syst., Man, Cybern., Syst.*, to be published.
- [38] D. Zhang, "A genetic algorithm for the sensor location problem," M.S. thesis, Dept. Ind. Eng., Univ. Louisville, Louisville, KY, USA, 2011.
- [39] Z. Hong and D. Fukuda, "Effects of traffic sensor location on traffic state estimation," *Proc. Soc. Behav. Sci.*, vol. 54, pp. 1186–1196, Oct. 2012.
- [40] J. Zhang, X. Zhang, and J. Wu, "Genetic simulated annealing algorithm for optimal deployment of flow monitors," in *Proc. 3rd Int. Conf. Nat. Comput.*, Haikou, China, 2007, pp. 398–402.
- [41] C. Liu, "Efficient heuristic for placing monitors on flow networks," in *Proc. 7th Int. Symp. Parallel Architect. Algorithms Program.*, Nanjing, China, 2015, pp. 1–5.
- [42] R. Minguez, S. Sánchez-Cambronero, E. Castillo, and P. Jiménez, "Optimal traffic plate scanning location for O/D trip matrix and route estimation in road networks," *Transp. Res. B Methodol.*, vol. 44, no. 2, pp. 282–298, Feb. 2010.
- [43] I. Vlasenko, I. Nikolaidis, and E. Stroulia, "The Smart-Condo: Optimizing sensor placement for indoor localization," *IEEE Trans. Syst., Man, Cybern., Syst.*, vol. 45, no. 3, pp. 436–453, Mar. 2015.
- [44] J. Sun and Z. Li, "Development and implementation of a wheeled inverted pendulum vehicle using adaptive neural control with extreme learning machines," *Cognitive Comput.*, vol. 7, no. 6, pp. 740–752, 2015.
- [45] Z. Zhang, Z. Li, Y. Zhang, Y. Luo, and Y. Li, "Neural-dynamic-method-based dual-arm CMG scheme with time-varying constraints applied to humanoid robots," *IEEE Trans. Neural Netw. Learn. Syst.*, vol. 26, no. 12, pp. 3251–3262, Dec. 2015.
- [46] J. A. Bondy and U. S. R. Murty, *Graph Theory*. Berlin, Germany: Springer, 2008.
- [47] A. Bretto, *Hypergraph Theory*. Cham, Switzerland: Springer, 2013.
- [48] F. Harary and R. Z. Norman, "Some properties of line digraphs," *Rendiconti del Circolo Matematico di Palermo*, vol. 9, no. 2, pp. 161–168, Feb. 1960.

Yu Kang, photograph and biography not available at the time of publication.

Zerui Li, photograph and biography not available at the time of publication.

Yunbo Zhao, photograph and biography not available at the time of publication.

Jiahu Qin, photograph and biography not available at the time of publication.